Journal of Magnetics 7(1), 4-8 (2002)

Spin Transport in a Ferromagnet/Semiconductor/Ferromagnet Structure: a Spin Transistor

W. Y. Lee* and J. A. C. Bland[1]

Nano Device Research Center, Korea Institute of Science and Technology, Seoul 136-792, Korea
[1]Cavendish Laboratory, University of Cambridge, Cambridge CB3 0HE, UK

(Received 15 February 2002)

The magnetoresistance (MR) and the magnetization reversal of a lateral spin-injection device based on a spin-polarized field effect transistor (spin FET) have been investigated. The device consists of a two-dimensional electron gas (2DEG) system in an InAs single quantum well (SQW) and two ferromagnetic ($Ni_{80}Fe_{20}$) contacts: an injector (source) and a detector (drain). Spin-polarized electrons are injected from the first contact and, after propagating through the InAs SQW are collected by the second contact. By engineering the shape of the permalloy contacts, we were able to observe distinct switching fields (H_c) from the injector and the collector by using scanning Kerr microscopy and MR measurements. Magneto-optic Kerr effect (MOKE) hysteresis loops demonstrate that there is a range of magnetic field (20~60 Oe), at room temperature, over which the magnetization in one contact is aligned antiparallel to that in the other. The MOKE results are consistent with the variation of the magnetoresistance in the spin-injection device.

Key words : Spin transport, spin transistor, spin-injection device, spin FET

1. Introduction

A new paradigm of electronics based on the spin degree of freedom of the electron has recently attracted considerable scientific and technological interest due to the potential advantages of nonvolatility, speed, power consumption, and integration densities [1]. In particular, it is believed that spin-polarized electron transport in semiconductors where ferromagnetic thin films are used to inject an imbalance of spin-polarized electrons opens an opportunity towards a novel class of spin-based electronic devices, spintronic devices [1, 2]. Intensive work has been done on the injection of spin-polarized electrons from a ferromagnetic metal into a nonmagnetic metal, inducing interesting effects associated with spin accumulation [3, 4]. The bipolar spin transistor consisting of a paramagnetic metal film sandwiched between two ferromagnetic metals by Johnson [3] is a device based on spin injection, offering a spin switch storage element in a nonvolatile solid-state memory array. Since Prinz [5] demonstrated that high-quality ferromagnetic metal films can be grown on semiconductors, it has been expected that such a hybrid metal/semiconductor spin transistor could be integrated with semiconductor technology. However, few investigations of spin-polarized transport in ferromagnet-semiconductor systems exist, and the spin transistor is still far from applications in the complementary metal oxide semiconductor (CMOS) industry.

Datta and Das [2] proposed the idea of a spin-polarized field effect transistor (spin FET), which would apply the spin-injection concept to ferromagnetic films on semiconductors, in particular, a two-dimensional electron gas (2DEG), as shown in Fig. 1. In such a device, the current modulation results from the spin precession, which can be altered by an effective electric field due to the spin-orbit coupling in narrow band-gap semiconductors, and ferromagnetic contacts are used to inject and detect spin-polarized electrons. Nitta *et al.* [6] pursued the injection of spin-polarized carriers into a two dimensional electron gas (2DEG) channel which had been formed at a compound semiconductor heterostrucuture interface, demonstrating that the spin-orbit interaction could be controlled by applying a gate voltage. Hammar *et al.* [7] observed spin injection at a ferromagnet/2DEG interface by projecting the spin-polarized current of the ferromagnet,

*Corresponding author: Tel: +82-2-958-5428,
Fax: +82-2-958-6851, e-mail: wylee@kist.re.kr

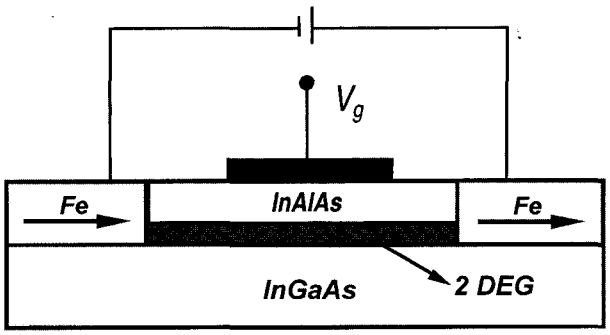

Fig. 1. Spin-polarized field effect transistor (spin FET) based on theoretical idea proposed by Datta and Das, which applies the injection of spin-polarized carriers from a ferromagnetic metal into a two-dimensional electron gas (2DEG) channel.

demonstrating that reversing the magnetization orientation of the ferromagnet modulates the interface resistance. However, spin injection at a ferromagnet/2DEG interface still remains a controversial and challenging work, due to the local Hall effect on a low-density 2DEG [8] and due to a basic obstacle to spin injection from a ferromagnetic metal emitter into a semiconductor originating from the conductivity mismatch between these materials [9].

In the present work, we investigated the spin-polarized transport related to the magnetization reversal of the two ferromagnetic ($Ni_{80}Fe_{20}$) contacts, the source and the drain, in a spin FET based on a ferromagnet/2DEG/ferromagnet structure. Kerr microscopy demonstrates distinct switching fields (H_c) in the two permalloy contacts, allowing the magnetizations of the contacts to be aligned antiparallel to each other. These results are discussed in association with the magnetotransport measurements in lateral spin-injection devices.

2. Experiment

In the sample, a two dimensional electron gas (2DEG) was provided by a 150-Å-wide InAs single quantum well with AlSb barriers. The top AlSb barrier layer was protected from oxidation by a 50-Å GaSb layer. Ferromagnetic contacts ($Ni_{80}Fe_{20}$: *A*, *B*) were deposited in the middle part of a Hall bar, as shown in Fig. 2(a). The contacts were defined by electron beam lithography and contacted to the external circuitry with a network of extended NiCr/Au contacts patterned by optical lithography. The connections of contacts *A* and *B* with the extended NiCr/Au contacts were also made from permalloy. However, it should be noted that only the contacts *A* and *B* were in contact with the semiconductor surface. The rest were isolated from the surface with a layer of polyamide which

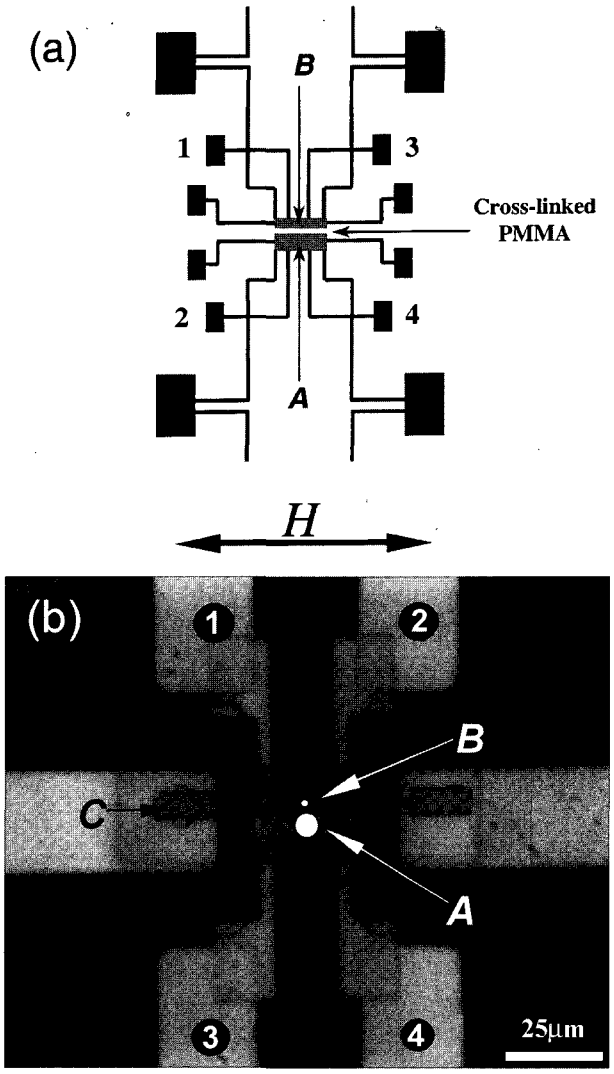

Fig. 2. (a) Schematic diagram of the device and (b) optical micrograph showing permalloy contacts *A* and *B*. The connections between the contacts *A* and *B* with the extended NiCr/Au are also shown. *C* indicates a contact pad, which is a part of the structures connecting with NiCr/Au contacts for MR measurements. The dots on the center of the contacts denote approximate laser beam spot size for MOKE measurements.

was deposited on the device, except for a window where the ferromagnetic contacts were located. The ferromagnetic contacts were deposited by evaporation of permalloy ($Ni_{80}Fe_{20}$). Contact *A* was 5 μm wide and 25 μm long and the contact *B* was 1 μm wide and 30 μm long, and both were 500 Å thick. A 200 Å thick layer of Au was deposited on the top of the permalloy contacts in order to protect them from oxidation. The distance between two parallel contacts was 1 μm.

To ensure a good ohmic contact between the ferromagnetic contacts and the InAs layer, we selectively etched

away the top GaSb and AlSb layers in the area under the contacts by dipping the sample in MF319 developer [10] prior to the deposition of the contacts. This process was followed by brief dipping in $(NH_4)_2S$. This removed any oxide, which could act as a spin scatterer due to the paramagnetic nature of oxygen from the surface of the InAs under the contacts. It also passivated the InAs surface with sulphur and decelerates the oxidation process of InAs [11]. Within 5 minutes of passivation, the sample was inserted in an evaporator for the deposition of the permalloy contacts. Finally, the exposed window in the polyamide was covered with cross-linked polymethylmethacrylate (PMMA).

Micron-scale magneto-optic Kerr effect (MOKE) studies were performed to assess the magnetization reversal in the two permalloy contacts. MOKE measurements are necessary to ensure the switching behavior of the magnetic contacts. Magnetoresistance (MR) measurements are ambiguous, because several mechanisms can give rise to an MR response. MOKE hysteresis loops were obtained at room temperature by using scanning Kerr microscopy [12]. Two objective lenses (× 20, Numerical Aperture: 0.55, × 50, NA: 0.85) were used to focus the probing laser beam (~4 μm, ~1 μm spot sizes, respectively) on the permalloy contacts. Figure 2(b) displays an optical photograph showing the two permalloy contacts *A* and *B*. The connections between the contacts *A* and *B* and the extended NiCr/Au are also shown. The dots in the center of the contacts denote the approximate laser beam spot size. MR measurements were performed in an applied magnetic field parallel to the 2DEG and along the long axis of the permalloy contacts *A* and *B* at temperatures from 300 mK to 10 K. A constant ac current of 1 μA was applied between positions ① and ②, and the voltage drop between positions ③ and ④ was recorded by using lock-in amplification techniques, as seen in Fig. 2(b). The variation in the magnetoresistance is defined as $\Delta R=R_H-R_{H=0}$, where R_H is the resistance at a given magnetic field.

3. Results and Discussion

The two permalloy contacts have been designed to show two different switching fields, ensuring that at certain magnetic fields they are magnetized either parallel or antiparallel to each other. An examination of the magnetization reversal behavior of the two permalloy contacts was carried out to confirm the effect by using the magneto-optic Kerr effect (MOKE). Figure 3 shows the microscopic MOKE hysteresis loops obtained when the magnetic fields were applied parallel to the long axis of the contacts *A* and *B*, indicating that the wire axis is the

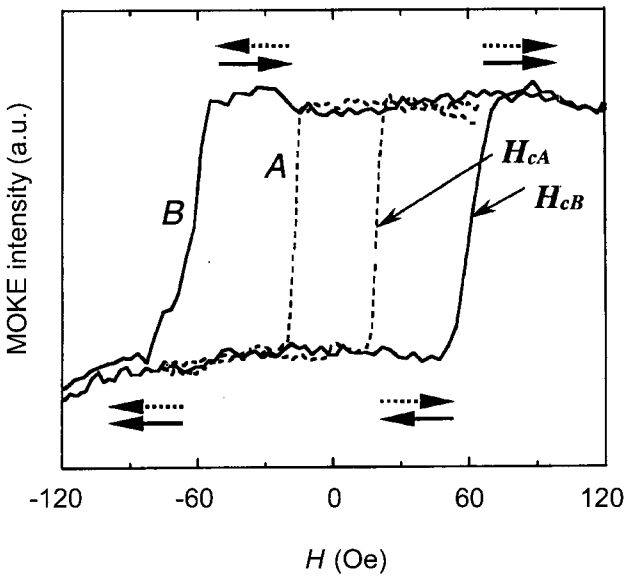

Fig. 3. Microscopic MOKE hysteresis loops for permalloy contacts *A* (dashed line) and *B* (solid line) measured by scanning Kerr microscopy at room temperature. The arrows denote parallel and antiparallel orientations of the contacts *A* and *B*, corresponding to H_{cA} and H_{cB}, respectively.

easy direction of the magnetization and that there are two distinct switching fields (H_{cA} = 20 Oe, H_{cB} = 60 Oe), one in the hysteresis loop for contacts *A* and the other in the loop for *B*. These results are in qualitative agreement with previous work [13], demonstrating that permalloy wires have their easy axis of magnetization along the long axis of the wire due to the magnetic shape anisotropy, and that a marked increase in the easy-axis switching field is observed as the wire width decreases. This is due to buckling of the magnetization perpendicular to the wire, leading to the formation of domain walls perpendicular to the wire [13, 14]. These walls prevent reverse domains from moving along the wire when the wire width is smaller than the buckling wavelength. It is unlikely that the domain configuration of contacts *A* and *B* in a zero applied field is a single domain due to edge domains which dominate switching behavior in ferromagnetic rectangular elements [15].

The MOKE hysteresis loops for the contacts (*A*, *B*) are compared with that of a contact pad [5×15 μm^2, *C* in Fig. 2(b)] which is a part of the structure connecting with the NiCr/Au contacts for MR measurements and which shows a much smaller switching field ($H_c \approx 3$ Oe). Our previous work [12] demonstrated that the hysteresis loop from a focused beam on the center of a ferromagnetic wire represents the wire's magnetic properties, except for the edge areas, where the spatial variation in the demagnetizing field is significant due to free poles. That work

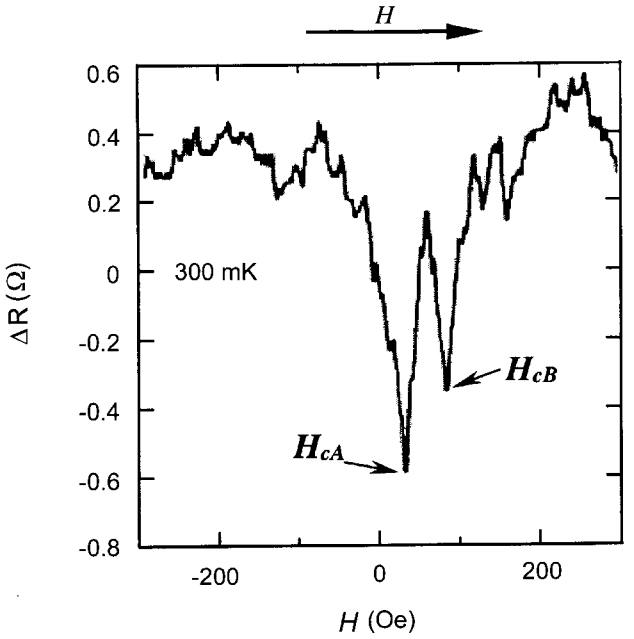

Fig. 4. Variation in the magnetoresistance (ΔR) between permalloy contacts *A* and *B*. The arrow shows the direction of the sweeping magnetic field.

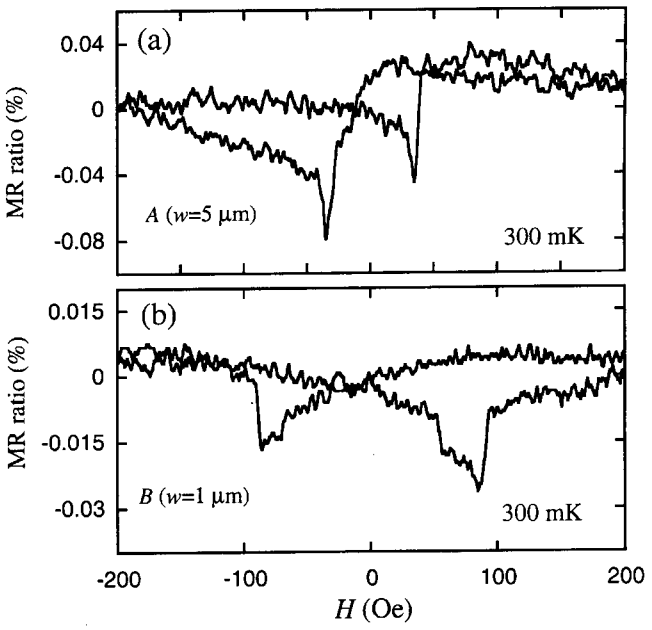

Fig. 5. Variation in the anisotropic magnetoresistance of (a) permalloy contact *A* and (b) contact *B*, respectively, when a magnetic field is swept up along the long axis of the contacts.

also demonstrated that the junction is crucial in determining the magnetization reversal and switching field [12]. In fact, the switching fields at the junctions in the device, which was formed by the electrode ($Ni_{80}Fe_{20}$) and the perpendicular arm ($Ni_{80}Fe_{20}$), were found to be smaller than those in the center of the two contacts. Nevertheless, it is clear from Fig. 3 that such a design provides the contacts (*A*, *B*) with two distinct switching fields between which the magnetization in one contact is aligned antiparallel to that in the other. In Fig. 3, the arrows represent parallel and antiparallel orientations of the magnetizations of the contacts (*A*, *B*). The MOKE hysteresis results show directly that there is a range of magnetic fields (20~60 Oe) in the device where the magnetizations of contacts *A* and *B* are antiparallel with respect to each other.

Figure 4 shows the variation in the magnetoresistance (ΔR) of the spin injection device measured at 300 mK when a magnetic field is swept up along the long axis of the permalloy contacts. Striking peaks were found at 35 Oe and 85 Oe, respectively. This shows the switching of the polarization of the electron spin in the device for certain magnetic fields, corresponding to the switching fields of the magnetizations of the two permalloy contacts. Four-terminal magnetoresistance measurements of the permalloy contacts *A* and *B* themselves were also carried out at 300 mK as shown in Fig. 5. The minimum resistance, which corresponds to the coercive field, was observed in the anisotropic MR curves of the two contacts and was in good agreement with the peaks in the MR curve of the device, as shown in Fig. 4.

From the weak antilocalization observed in the four-terminal magnetoresistance measurements near zero field in the InAs 2DEG system, it is possible to estimate a spin dephasing length (l_{sd}) for the electrons in the device. These measurements were made on a standard Hall bar without magnetic contacts in magnetic fields applied perpendicular to the 2DEG. Weak antilocalization in such structures is caused by spin splitting of the conduction band, which is the predominant cause of spin dephasing [16]. Using the fitting method described in Ref. 16, Gardelis *et al.* [17] estimated the spin dephasing time (τ_{sd}) to be ~9 ps. Using the mobility $\mu = 4.9\ m^2sec^{-1}V^{-1}$, the electron density $n_s = 6 \times 10^{15} m^{-2}$ calculated from the Shubnikov-de-Haas oscillations of the four-terminal magnetoresistance and the effective mass $m = 0.04m_o$ (m_o = electron rest mass) for InAs [18], the spin dephasing length (l_{sd}) was calculated as 1.8 μm. For the calculations, we used the expression $l_{sd} = (l\upsilon_F t_s)^{1/2}$, where l is the elastic mean free path and υ_F the Fermi velocity in the system. Although the spin diffusion length is comparable to the distance (1 μm) between the permalloy contacts, ΔR/R is only 0.2%. The most likely reason for such a small value of ΔR/R is that the electrons leaving one contact and entering the next can have a variety of different path lengths. Thus, an average signal is measured for the

electrons which have undergone different degrees of precession. However, only a small percentage of the electrons propagate without spin scattering contributing to the observed signal.

The observed change in the magnetoresistance (ΔR) in the device can be given by

$$\Delta R = \Delta R_A + \Delta R_B + \Delta R_{CA} + \Delta R_{CB} + \Delta R_S, \quad (1)$$

where ΔR_A and ΔR_B are the magnetoresistance changes of the permalloy contacts *A* and *B*, respectively. ΔR_{CA} and ΔR_{CB} are those of the interfaces between the semiconductorand the contacts *A* and *B*, respectively. ΔR_S results from electrons propagating from the first permalloy contact to the second without spin scattering. We found that ΔR_A and ΔR_B were much smaller than ΔR. Thus, these contributions are negligible. Therefore, in order to explain the observed signal, we took only the contributions from the interface contacts ($\Delta R_{CA} + \Delta R_{CB}$) and the InAs ($\Delta R_S$) into consideration. If the zero-spin splitting in InAs and the fact that it is diamagnetic are considered, the contribution from the interface contacts is a maximum when the magnetizations in both ferromagnetic contacts are antiparallel to the spin orientation in the InAs 2DEG, and it is a minimum when the magnetizations in the two ferromagnetic contacts is parallel to the spin orientation in the InAs. ΔR_S, however, is a minimum when both permalloy contacts are magnetized parallel to each other, and it is a maximum between the two coercive fields where the magnetizations of the two contacts are antiparallel to each other. The observed signal is the sum of these two contributions.

4. Conclusion

The spin transport related to the magnetization reversal in a lateral spin-injection device with an InAs two-dimensional electron gas (2DEG) and two ferromagnetic ($Ni_{80}Fe_{20}$) contacts placed 1 μm apart has been investigated. It is found that spin-polarized electrons are injected from the first ferromagnetic contact, and propagate through the InAs, and are collected by the second contact. Magneto-optic Kerr effect (MOKE) hysteresis loops demonstrate that there is a range of magnetic fields (20~60 Oe) over which the magnetization in one contact is aligned antiparallel to that in the other. The MOKE results are consistent with the variation of the magnetoresistance. There are two contributions to the magnetoresistance. The first is an interface resistance between the ferromagnet and the semiconductor, resulting from the zero spin splitting in InAs. The second results from spins propagating from one ferromagnetic contact to the next contact. This is a maximum between the switching fields of the two permalloy contacts.

Acknowledgments

This work was supported by the KRCF (Quantum Dots-Functional Devices) and Korea Ministry of Science and Technology (National program for Tera-level Nanodevices).

References

[1] G. Zorpette, *IEEE Spectrum* **38**, 30 (2001); S. A. Wolf, D. D. Awschalom, R. A. Buhrman, J. M. Daughton, S. von Molnar, M. L. Roukes, A. Y. Chtchelkanova, and D. M. Treger, *Science* **294**, 1488 (2001).

[2] S. Datta and B. Das, *Appl. Phys. Lett.* **56**, 665 (1990).

[3] M. Johnson, *Science* **260**, 320 (1993); *Phys. Rev. Lett.* **70**, 2142 (1993); *J. Mag. Mag. Mater.* **140-144**, 21 (1995).

[4] A. Fert and S. F. Lee, *J. Mag. Mag. Mater.* **165**, 115 (1997).

[5] G. A. Prinz, *Science* **250**, 1092 (1990).

[6] J. Nitta, T. Akazaki, H. Takayanagi, and T. Enoki, *Phys. Rev. Lett.* **78**, 1335 (1997).

[7] P. R. Hammar, B. R. Bennett, M. J. Yang, and M. Johnson, *Phys. Rev. Lett.* **83**, 203 (1999).

[8] F. G. Monzon, H. X. Tang, and M. L. Roukes, *Phys. Rev. Lett.* **84**, 5022 (2000); B. J. van Wees, *Phys. Rev. Lett.* **84**, 5023 (2000).

[9] G. Schmidt, D. Ferrand, L. W. Mollenkamp, A. T. Filip, and B. J. van Wees, *Phys. Rev. B* **62**, R4790 (2000).

[10] C. Gatzke, S. J. Webb, K. Fobelets, and R. A. Stradling, *Semic. Sci. Techn.* **13**, 399 (1998).

[11] H. Oigawa, J. F. Fan, Y. Nannichi, H. Sugahara, and M. Oshima, *Jpn. J. Appl. Phys.* Pt2-Letters **30**, L322 (1991).

[12] W. Y. Lee, C. C. Yao, A. Hirohata, Y. B. Xu, H. T. Leung, S. M. Gardiner, S. McPhail, B. C. Choi, D. G. Hasko, and J. A. C. Bland, *J. Appl. Phys.* **87**, 3032 (2000).

[13] A. O. Adeyeye, G. Lauhoff, J. A. C. Bland, C. Daboo, D. G. Hasko, and H. Ahmed, *Appl. Phys. Lett.* **70**, 1046 (1997).

[14] K. J. Kirk, J. N. Chapman and C. D. W. Wilkinson, *Appl. Phys. Lett.* **71**, 539 (1997).

[15] J. Shi, S. Tehrani, T. Zhu, Y. F. Zheng, and J. G. Zhu, *Appl. Phys. Lett.* **74**, 2525 (1999).

[16] G. L. Chen, J. Han, S. Datta, and D. B. Janes, *Phys. Rev. B* **47**, 4084 (1993).

[17] S. Gardelis, C. G. Smith, W. Y. Lee, E. H. Linfield, and J. A. C. Bland, *Physica E: Low-dimensional systems and nano-structures* **6**, 718 (2000).

[18] E. I. Rashba, *Sov. Phys. Solid States* **2**, 1109 (1960).